



## Basic thermodynamics of FLOXCOM, the low- $\text{NO}_x$ gas turbines adiabatic combustor

Yeshayahou Levy \*, Valery Sherbaum, Patric Arfi

*The Turbo and Jet Engine Laboratory, Faculty of Aerospace Engineering, Technion, Israel Institute of Technology, Haifa 32000, Israel*

Received 12 November 2003; accepted 21 November 2003  
Available online 17 January 2004

### Abstract

The FLOXCOM Project is aimed to develop technology for clean and efficient gas turbines, operating at high temperatures. It is based on the technologically innovative combustion solution—flameless oxidation. The investigation is directed towards the validation of engineering feasibility of the flameless oxidation technology for the production of operating pilot combustors that will demonstrate, advantages including among others, improved performance relating to low  $\text{NO}_x$  levels, maintaining uniform combustor wall temperatures, uniform fuel stream injection and more, resulting in an increased mean time between failure (MTBF) and reliability of the gas turbine. Combustion chambers for gas turbines and jet engines differ from conventional industrial furnace design by being “adiabatic” (without heat extraction inside the combustor) and by operating at elevated pressures. Consequently, the aero-thermodynamics of the internal flow requires a different approach. The present paper is concerned with the thermodynamic relationships of gas turbine flameless oxidation. A detailed analysis of the different operational scheme options is described.

It is shown that the thermodynamic process and operational parameters within the present low- $\text{NO}_x$  gas turbine combustor are principally different to those of industrial furnace operating in the flameless oxidation mode of combustion.

© European Communities, 2004. Published by Elsevier Ltd. All rights reserved.

**Keywords:**  $\text{NO}_x$ ; Combustion; Gas turbine; FLOXCOM; Pollution; Emission

\* Corresponding author. Tel.: +972-4-8293807; fax: +972-4-8121604.  
E-mail address: [levyy@aerodyne.technion.ac.il](mailto:levyy@aerodyne.technion.ac.il) (Y. Levy).

### Nomenclature

$A$	cross-section area (m <sup>2</sup> )
$C_p$	specific heat capacity (J/(kg K))
$K$	recirculation rate, $K = \dot{m}_r/(\dot{m}_{as} + \dot{m}_f)$
$\dot{m}$	mass flow rate (kg/s)
$O$	oxygen content (mass percentage)
$T$	temperature (K)
$V$	velocity (m/s)
$\lambda$	relative specific heat capacity, $C_p/C_{pa}$
$\theta$	relative temperature, $T/T_a$
$\mu_x$	relative mass flow rate, $\dot{m}_x/\dot{m}_a$
$\rho$	density (m <sup>3</sup> /kg)
$\Phi$	equivalence ratio

### Subscripts

a	air
c	combustion
e	exit
r	recirculation
s	stirred

## 1. Introduction

The pollutant formation processes in a gas turbine are associated with the combustor design and operational conditions [1–4,6,9,11,12]. The nature of pollutant formation is such that the concentrations of carbon monoxide and unburned hydrocarbons are highest at low-power conditions and diminish with increased power. In contrast, oxides of nitrogen and smoke are fairly insignificant at lower power settings and attain maximum values at the highest power condition. Characteristic trends are summarized in Table 1 and sketched in Fig. 1 for conventional gas turbines.

The thermal NO has an exponentially dependent on temperature. Thus, the reduction in temperature emerges as the main strategy for controlling thermal NO<sub>x</sub> emission from gas turbines.

Table 1  
Aircraft turbine engine emissions depending on operating conditions

Emission type	Primarily associated with engine operating at
H <sub>2</sub> O, CO <sub>2</sub> , SO <sub>x</sub>	All power settings
Smoke (C)	All power settings
CO	Low power, ground idle
UHC	Low power, ground idle
NO <sub>x</sub>	All power settings, increase with power

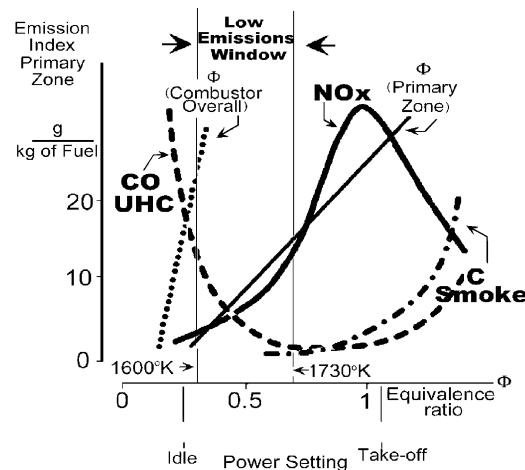


Fig. 1. Compromises involved between emitted species and the “low-emission window” (after [13]).

The second objective should be to eliminate the hot spots from the reaction zone. Indeed, there is little point in achieving a satisfactory low average temperature if the reaction zone contains localized regions of high temperatures in which the rate of  $\text{NO}_x$  formation remains high. Finally, the time available for the formation of  $\text{NO}_x$  should be kept to a minimum. Reduction of thermal NO by both the flame temperature and residence time reduction is readily accomplished by increasing the flow of air into the primary zone. However, the reduction of the  $\text{NO}_x$  emissions by reducing the reaction temperature and/or residence time can have an adverse effect on the combustion stability, the production of CO and UHC or even thermal efficiency. Prompt NO emissions can be reduced by (1) replacement of hydrocarbons by other fuels; (2) very lean combustion; or (3) very rich combustion in the primary zone. The presence of fuel bound nitrogen results in the formation of substantial quantities of fuel NO. The process is less temperature dependent than the thermal route and reduction of flame temperature does not markedly reduce nitric oxide formed in this way. Control of fuel NO is thus directed toward either utilization of fuel rich conditions that reduce fuel nitrogen components to molecular nitrogen or removal at the exhaust.

The requirement to simultaneously minimize all three  $\text{NO}_x$  formation rates without producing unacceptable levels of other pollutants still remains as a formidable task for which there is currently no simple solution. The effort in previous works, as well as in the one presented here, are mainly concentrated on reducing the main NO formation route i.e. thermal NO emissions. An overall understanding of the problems involved in combustor design for reducing all pollutant emissions simultaneously can be gained by referring to Fig. 2 in which the emissions of CO and  $\text{NO}_x$  are plotted against primary zone temperatures for a hypothetical conventional combustor. This figure shows that too much CO is formed at temperatures below 1600 K, while excessive amounts of  $\text{NO}_x$  are produced at temperatures higher than 1730 K. Only in the fairly narrow band of temperatures are the levels of both CO and  $\text{NO}_x$  below mandated values. This region is referred as *the low-emission window*. The underlying principle of all the technical approaches, described in the next chapter, is that of maintaining the combustion zone (or zones) within a fairly narrow range of temperatures over the entire power range of the engine.

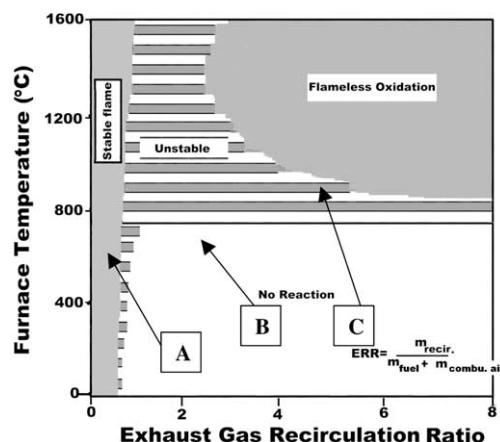


Fig. 2. Schematic of flame stability limits (from [15]) (temperatures are relative to ambient).

## 2. Flameless oxidation

The present work selected a promising combustion concept based on internal flue gas recirculation. As stated earlier, flue gas recirculation is efficient in  $\text{NO}_x$  reduction but limited by the maximal quantity of recirculated gas since in normal ambient air vitiation may lead rapidly to blow-off [4,5]. Nevertheless, it was experimentally found by Wüning [14] that under special conditions, a stable form of combustion is possible for high recirculation rates of exhaust gases. Note that here only exhaust gas recirculated into combustion air and fuel, before the reaction flame front, is considered to be recirculated exhaust gas. The recirculation of hot products into the flame to improve flame stabilization is not considered as recirculated exhaust gas.

Fig. 2 shows a schematic diagram of the stability limits for different combustion modes. Concerning FGR, stable flames (zone A) are possible over the whole range of combustion chamber temperature if air is not vitiated providing that sufficient amount of combustion products are recirculated for flame stabilization. At ambient temperature this conventional combustion regime is limited for recirculation rates up to low exhaust recirculation rates ( $\text{ERR} = 0.3$ ). For higher recirculation rates, the flame becomes unstable (zone B), as already observed in many experimental works, the flame lift-off and finally blowout. However, if the temperature of air is high enough, the recycling rate may become large (here around  $\text{ERR} = 2.5$ ) and the fuel can react in a very steady, stable form of flameless oxidation (zone C).

It was suggested by Wüning [14] that if the diluted air temperature exceeds the fuel auto-ignition temperature, the fuel ignites automatically and continuous combustion is sustained. Auto-ignition temperatures of gaseous fuels are dependent on kinds of fuel and concentration of oxygen of the diluted air. It therefore appears experimentally that a stable combustion domain exists for high ratio of exhaust gas recycling. Under ideal conditions, such combustion was reported to takes place without any visible or audible flame, for that reason it was named flameless oxidation [15]. It has also been reported that the flame never emitted bright emission. It is important to note that conditions for flameless oxidation are conditions in which ordinary combustion can *not* be sustained with ambient temperature combustion air.

To explain the observation of Wünnig [14], it is interesting to consider the combined effect of high temperature air and increased inert content of a mixture on flame stability. Katsuki and Hasegawa [2] observed that for a diffusion flame the conditions for flame stabilization are such that the temperature of the inlet gases has to be increased if the oxygen concentration is lowered. Actually, very diluted air with oxygen content as low as 3% can sustain combustion when it is preheated up to 1200 K.

### 3. Flameless oxidation characteristics

The main characteristic of the flameless oxidation mode is the uniform thermal field obtained. The presence of exhaust gas recirculation, at high recirculation rates, reduces the temperature rise during the reaction by a few hundred degrees. In addition, it was shown that the influence of air preheating on  $\text{NO}_x$  emissions became small with increased dilution. Steep gradients and large temperature and concentration differences are characteristic of flame combustion whereas the flameless oxidation mode is much more homogeneous. The heat release due to combustion reaction is distributed, yielding a dispersed and moderate temperature rise. In contrast to the diffusion flame, no high gradients of temperature and species concentration are observed. The temperature profiles of flameless oxidation are lower than in non-diluted diffusion flames and uniformly distributed. The principal advantage is that by avoiding peak temperatures, the thermal NO formation can be largely suppressed, even at the highest air temperatures.

The present work proposes a new application of flameless oxidation to an adiabatic system typical of gas turbine combustor. The ultimate goal of the study is to provide an innovative gas turbine combustor combustion method for high operating temperatures and pressures capability, which can reduce both fuel consumption and  $\text{NO}_x$  emission.

### 4. Fundamentals of thermodynamics parameters of the present flameless oxidation combustor

Several schemes of the adiabatic combustion with a high recirculation rate of the combustion products were considered. The analysis considers a schematic construction of a combustor that includes the following modules [7]; an inlet for the fresh air that can be split into different air streams; a combustion section that consist of fuel inlet and a large toroidal vortex and an exhaust section. Two mixing section exists; between air stream and combustion products, directing the mixture into the combustion zone and between combustion products and another air stream, directing the mixed gases to the combustor outlet. It seems that there are only three possible different schemes of the adiabatic combustion: (a) Splitting the air inlet to two fractions: one is stirred with a portion of the combustion products of the recirculation zone. This mixture is recycled to the combustor. The other one dilutes the combustion products till the required exhaust temperature and is directed to the turbine, it was named as combustor of type “A”; (b) Part of the fresh air is stirred with the all combustion products. A portion of this mixture is recycled to the combustor and the other is diluted by the other part of the fresh air and is then directed to the turbine, it was named as combustor of type “B”; (c) This scheme is a combination of the previous two mentioned schemes, this option named as combustor of type “C”. Assuming perfect

combustion (100% efficiency), a calculation procedure for the thermodynamic parameters and the oxygen mass fraction at every point of the combustion is demonstrated. Based on this study the performance of the FLOXCOM<sup>1</sup> combustor is calculated. Detailed calculation for the type “A” combustor is performed as an example. Wünnig [14] pointed out that only exhaust gas recirculating into combustor before the reaction flame front could be considered as recirculating gas. The recirculation of hot products into the flame to improve flame stabilization is not considered as the recirculating gas. Fig. 2 shows a schematic diagram of the stability limits for different combustion modes. The author did not provide any information about the oxygen mass fraction inside of the recirculation zone, even though it is one of the principal data of the flameless oxidation. To obtain the flameless oxidation and the associated low-NO<sub>x</sub> emissions, a critical requirement is to avoid direct combustion before the dilution of air with burnt gases. Intense mixing of air with a significant amount of the burnt gases before combustion is essential and therefore mixing must be enhanced in the preparation process prior to combustion.

To date, only non-adiabatic systems of the furnace type have been considered. Heat absorption by heated materials in the furnace as well as heat losses that exist in practical systems are influencing factors in defining the gas temperature in the furnace and consequently the temperature of the recirculated gas. The reduced temperature level of burnt gases as well as recycling flow rate largely affect the flame temperature. In such non-adiabatic systems the flame temperature can be controlled, keeping the global equivalence ratio constant by varying the preheat air temperature and the recycling rate of burnt gases and the internal heat absorption. Contrary to this, in the case of an adiabatic combustor [8], the thermodynamic parameters of the recirculating and the exhausting gases are determined by aerodynamic and thermodynamic processes inside the combustor only.

The following model describes some principal relationships of the internal thermodynamics and enables to evaluate the conditions required to achieve flameless oxidation in an adiabatic combustion system. The FLOXCOM combustor, is considered as an example and a procedure of calculation of thermodynamic parameters, mass flow rate, and oxygen content at every stage of the FLOXCOM combustor is described.

## 5. Optional schemes for an adiabatic flameless oxidation (FLOXCOM) combustor

Two principal schemes of the internal flow inside of the FLOXCOM combustor are considered in scheme “A” (Fig. 3) fresh air is split at the junction 1. One part of the fresh air,  $m_{as}$  is stirred

<sup>1</sup> FLOXCOM is an European funded FP5 Contract No. ENK5-CT-2000-00114 and is performed by a Consortium of eight partners, namely:

Israel Institute of Technology (Technion)—the Coordinator	IL
Imperial College of Science Technology & Medicine (ICSTM)	UK
CINAR Ltd. (CINAR)	UK
Instituto Superior Tecnico (IST)	P
Institute of Fundamental Technological Research (IPPT-PAN)	PL
ANSALDO Ricerche Srl. (Ansaldo)	I
B&B AGEMA GmbH (B&B-AGEMA)	DE
Rheinisch-Westfälische Technische Hochschule (RWTH)	DE
Ansaldo Caldaie (CCA)	I

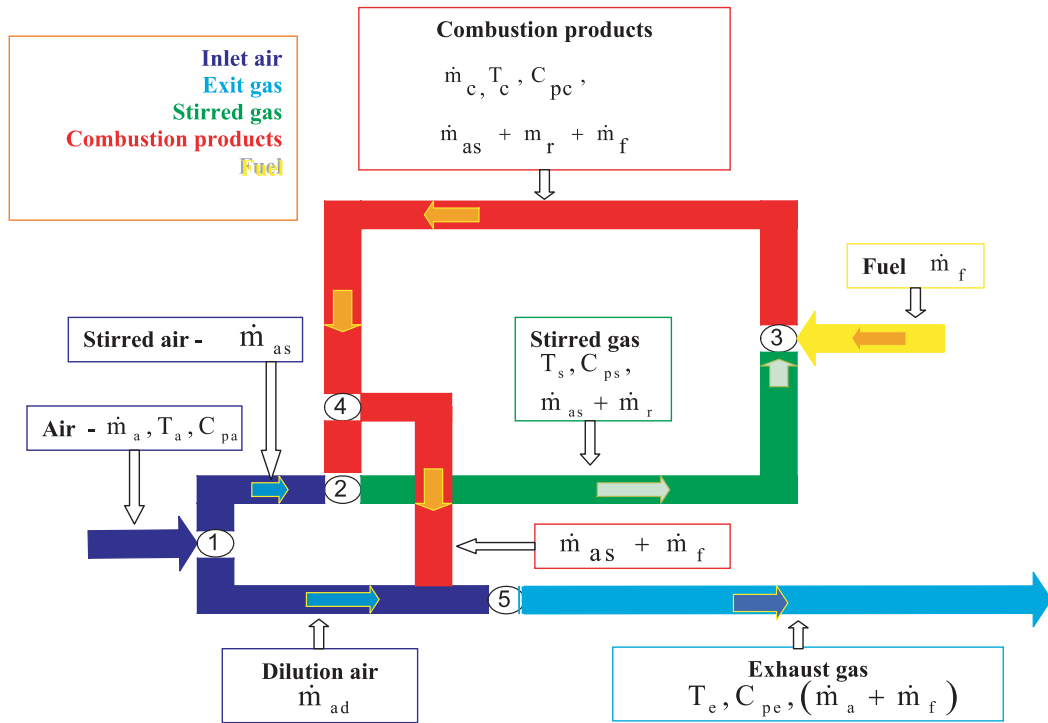


Fig. 3. Scheme A (air is mixed with the combustion products,  $T_e$  and  $T_s$  are independent each from other).

with the combustion products,  $m_r$ , at the junction 2. Fuel is injected to this mixture ( $m_r + m_{as}$ ) at junction 3. After mixing with fuel, combustion occurs. At junction 4, the combustion products,  $m_r + m_{as} + m_f$ , are split; one portion,  $m_r$ , returns to combustor through the junction 2 and the other,  $m_{as} + m_f$ , is mixed with the dilution air,  $m_{ad}$ , and is exhausted from the combustor. Scheme “B” differs from scheme “A” in the fact that the stirring air,  $m_{as}$ , is initially stirred with the combustion products,  $m_r + m'_{as} + m_f$ , (junction 2) and thereafter the mixture,  $m_r + m'_{as} + m_f + m_{as}$ , is split at the junction 3; one part,  $m_r + m'_{as}$ , returns to the combustor and the other is diluted by fresh air,  $m_{ad}$ , and is exhausted from the combustor. Schematic drawing of the possible combustor aerodynamics for scheme A is shown in Fig. 4. Scheme “B” differs in points 2 and 4: where the combustion products are mixed with stirring air and thereafter the mixture is mixed with the diluting air. It should be mentioned that both schemes are extreme cases of the adiabatic combustor with high recirculation rate. The real practical process is located in between and will be considered later.

## 6. Heat, mass and oxygen balance

In the following, the major assumption for the calculations are given:

- Inlet air temperature  $T_a$ , inlet mass flow rate  $m_a$ , combustion and exit temperatures  $T_c$  and  $T_e$  respectively, recirculation rate  $K$  and fuel properties are considered as prescribed values.

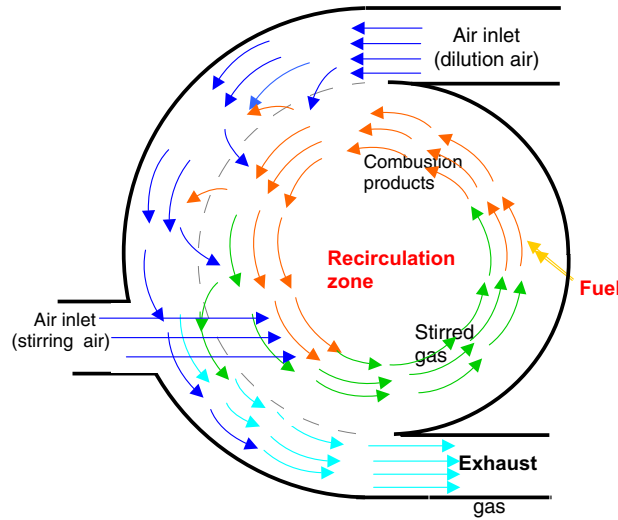


Fig. 4. Schematic drawing of the combustor locus, scheme A.

- A perfect adiabatic combustion is assumed.
- The initial fuel enthalpy in the heat balance is neglected.

Stirring air and dilution air mass flow rates, stirred gas mass flow rate, stirred gas temperature and oxygen percentage contents in every stage of the combustion must be found.

Combustor type “A” (see Figs. 3 and 4).

### 6.1. Heat and mass balance

The assumption is that here combustion products are mixed directly with part of the inlet air to form the exhaust mixture (no stirred gas in the exhaust gases). Therefore, stirred gas temperature  $T_s$  can be calculated from heat balance between air and combustion gases (junction 2):

$$C_{pa} \cdot T_a m_{as} + C_{pc} \cdot T_c \cdot m_r = C_{ps} \cdot T_s \cdot (m_r + m_{as}). \quad (1)$$

Taking into account notations for  $\theta$ ,  $\lambda$  and  $\mu$ , the expression for the relative stirred temperature may be written as

$$\theta_s = \frac{\mu_{as} + \lambda_c \cdot \theta_c \cdot \mu_r}{\lambda_s \cdot (\mu_r + \mu_{as})}. \quad (2)$$

According to definition of the recirculation rate

$$m_r = K \cdot (m_{as} + m_f), \quad \text{and so} \\ \mu_r = K \cdot (\mu_{as} + \mu_f).$$

Now the expression for the relative stirred gas temperature may be re-written in the following form:

$$\theta_s = \frac{\mu_{as} + \lambda_c \cdot \theta_c \cdot K \cdot (\mu_{as} + \mu_f)}{\lambda_s \cdot [(K + 1) \cdot \mu_{as} + K \cdot \mu_f]} = \frac{1 + \lambda_c \cdot \theta_c \cdot (K + \mu_f / \mu_{as})}{\lambda_s \cdot (K + 1 + K \cdot \mu_f / \mu_{as})} \quad (3)$$

One can see that minimal  $\theta_s = 1$  corresponds to recirculation ratio  $K = 0$  and maximal,  $\theta_s = \theta_c$ ,  $K = \infty$ . The dependences of stirring temperature on inlet parameters and combustion temperature are shown in Figs. 5 and 6 (the values from  $x$  were taken from Ref. [3]). One can see that even in low recirculation ratio, temperature before combustion can achieve stable combustion conditions.

The ratio  $\mu_f / \mu_{as}$  depends on  $\theta_s$  that is unknown. So as a first approximation value  $\theta_s$  may be calculated as an average magnitude between combustion temperature  $\theta_c$  and exit temperature  $\theta_e$ . After that it can be refined.

Ratio between air flow rate  $m_{ad}$ , that is required for dilution and between the air flow rate for the stirring gas  $m_{as}$  can be found from the following heat balance equation:

$$C_{pa} \cdot T_a m_{ad} + C_{pc} \cdot T_c \cdot (m_{as} + m_f) = C_{pe} \cdot T_e \cdot (m_{ad} + m_{as} + m_f). \quad (4)$$

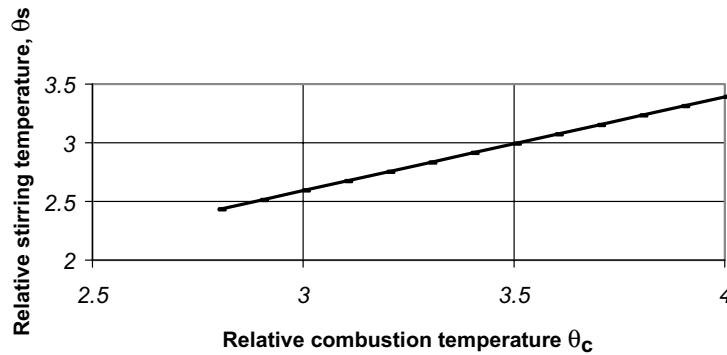


Fig. 5. Dependence relative stirring temperature on relative combustion temperature,  $K = 3$ .

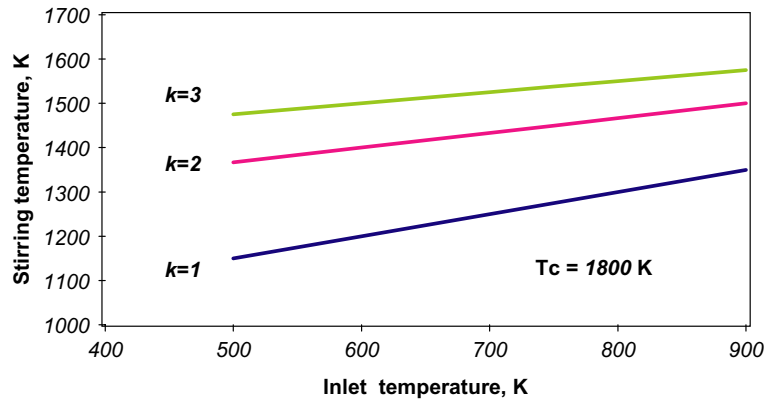


Fig. 6. Influence of inlet temperature and recirculation ratio on stirring temperature.

Taking into account notations for  $\theta$ ,  $\lambda$  and  $\mu$ , this equation may be written as

$$\mu_{ad}/\mu_{as} + \lambda_c \cdot \theta_c \cdot (1 + \mu_f/\mu_{as}) = \lambda_e \cdot \theta_e \cdot (\mu_{ad}/\mu_{as} + 1 + \mu_f/\mu_{as}). \quad (5)$$

Or,

$$\frac{\mu_{ad}}{\mu_{as}} = \frac{(\lambda_c \cdot \theta_c - \lambda_e \cdot \theta_e) \cdot (1 + \mu_f/\mu_{as})}{\lambda_e \cdot \theta_e - 1}. \quad (6)$$

This value does not depend on the recirculation ratio  $K$ .

Eqs. (3) and (6) enable to calculate stirred gas temperature and dilution air to stirred air ratio  $\mu_{ad}/\mu_{as}$ .

As total air mass flow rate  $m_a$  is a sum of stirred air and dilution air,

$$m_{ad} + m_{as} = m_a, \quad \text{so} \quad \mu_{ad} + \mu_{as} = 1,$$

their fractions can be written in the following way:

For stirring air fraction:

$$\mu_{as} = \frac{1}{1 + \mu_{ad}/\mu_{as}}. \quad (7)$$

For dilution air fraction:

$$\mu_{ad} = 1 - \mu_{as}. \quad (8)$$

The relative partition between the stirring and diluting air fractions are determined by the combustion temperature, inlet air temperature and the gas exit temperature and are not dependent neither on the recirculation rate nor on the stirred temperature. The values  $\mu_{as}$  and  $\mu_{ad}$  can be also found from the following considerations. As air is heated from  $T_a$  to  $T_e$ , relative fuel flow rate  $\mu_f$  can be calculated according to equivalence ratio  $\Phi_e$  and  $T_{as}$  (see for example [10, Fig. 20]). The value  $\mu_f/\mu_{as}$  may be found using similar considerations and according to the known heating from  $T_a$  to  $T_c$ . Thus,

$$\mu_{as} = \mu_f/(\mu_f/\mu_{as}) \quad \text{and, according to (8),} \quad \mu_{ad} = 1 - \mu_{as}.$$

## 6.2. Oxygen balance

Oxygen to the recirculation zone is supplied by the stirring air and its temperature rises from  $T_a$  till  $T_c$ . Equivalence ratio  $\Phi_c$  for such temperature increase may be found in [10, Fig. 20]. Mass percentage content of oxygen in the combustion product (after combustion) is

$$O_c (\%) = 23 \cdot (1 - \Phi_{as}) / (1 + \mu_f/\mu_{as}). \quad (9)$$

It is important, that content of oxygen in the combustion zone does not depend on  $K$ .

The percentage oxygen content in the stirred gas (before combustion) may be found from oxygen balance for the stirring zone:

$$O_c \cdot \dot{m}_r + 23 \cdot \dot{m}_{as} = O_s \cdot (\dot{m}_r + \dot{m}_{as}). \quad (10)$$

Taking into account the above relationship for the recirculation rate  $K$ , the percentage oxygen content in the stirred gas may be written through the relative mass flow rate values:

$$O_s = \frac{O_c \cdot K(1 + \mu_f/\mu_{as}) + 23}{(K + 1) + K \cdot \mu_f/\mu_{as}}. \quad (11)$$

Minimal value is  $O_s = O_c(1 + \mu_f/\mu_{as})$  and it corresponds to recirculation ratio  $K = \infty$  and maximal,  $O_s = 23$ ,  $K = 0$ .

The percentage of oxygen content at the exit of the combustor may be found from the equivalence ratio  $\Phi_e$  (according to the known combustion temperature rise and inlet air temperature [10, Fig. 20]:

$$O_e = 23 \cdot O_a \cdot (1 - \Phi_e)/(1 + \dot{m}_f/\dot{m}_a). \quad (12)$$

It is clearly seen that the oxygen percentage does not depends on the recirculation ratio. From the other hand, this value may be found from oxygen mass balance:

$$O_e \cdot (m_{as} + m_{ad} + m_f) = 23 \cdot m_{ad} + O_c \cdot (m_{as} + m_f).$$

Or, at the relative values

$$O_e = \frac{O_c \cdot (\mu_{as} + \mu_f) + 23 \cdot \mu_{ad}}{1 + \mu_f}. \quad (13)$$

It is obviously that results of Eqs. (12) and (13) must be identical and they may be used for oxygen balance checking. Figs. 7 and 8 show that oxygen content before combustion and even within the combustion products is much more than these values for industrial furnaces. This presents the main difference between low- $\text{NO}_x$  combustion process in industrial furnaces and within gas turbines.

In combustor type “B”, similar results should be obtained since the same initial conditions exists for air mass flow rate, the inlet temperature and the fuel flow rate.

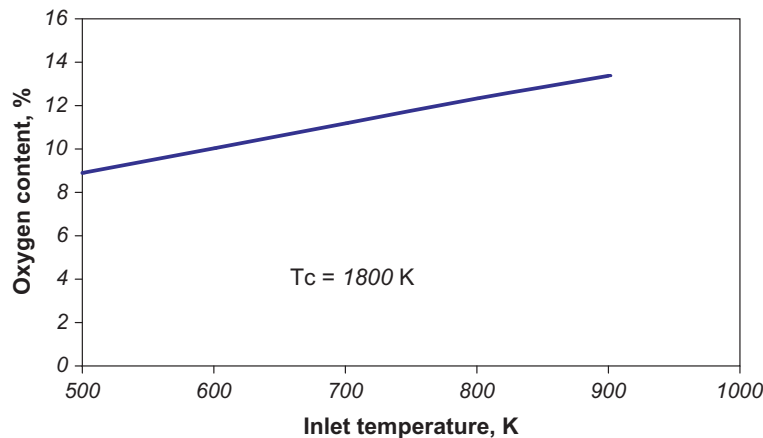


Fig. 7. The oxygen content at the combustion products as a function of inlet temperature.

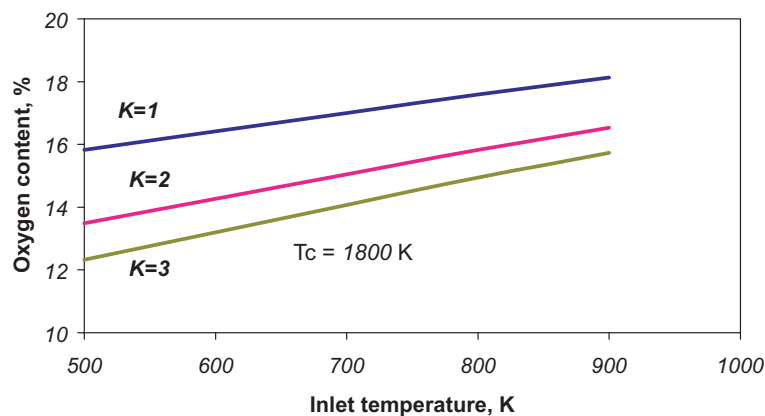


Fig. 8. Dependence oxygen mass content (%) within the stirring gas (before combustion) on the inlet temperature and recirculation ratio.

## 7. Conclusion

A review of the flameless oxidation combustion mode, relevant to gas turbines and jet engines is given. The adiabatic combustion with high internal recirculation rate was considered. Assuming perfect combustion (100% efficiency), a procedure for calculating the thermodynamic parameters and the gas properties, at the each stage of the combustion process, is developed. It is shown that, due to maximal combustion temperature restriction, the oxygen content remain at significant value. The oxygen content at the end of the combustion zone increases when the difference between combustion and air inlet temperature decreases. This is a significant feature of the present low- $\text{NO}_x$  combustion process. It is different to the conventional process in gas turbines where complete combustion is assumed in its primary zone. The model can be considered for preliminary estimation of thermodynamic parameters of the FLOXCOM combustor as well as its gross dimensions. It enables to obtain the initial data needed for further detailed study of the aerothermodynamic and chemical processes by CFD codes.

## Acknowledgements

The authors would like to thank the European commission for the financial support for this work, carried out with the European Union Funded Research, 5th Framework Programme, FP5 Contract No. ENK5-CT-2000-00114.

## References

- [1] D. Bradley et al., The mathematic modeling of lift-off and blow-off of turbulent non-premixed methane jet flames at high strain rates, in: 27-th Symposium (International) on Combustion, The Combustion Institute, Pittsburgh, 1998.
- [2] M. Katsuki, T. Hasegawa, The science and technology of combustion in highly preheated air, in: 27-th Symposium (International) on Combustion, The Combustion Institute, Pittsburgh, 1998, pp. 3135–3146.

- [3] H. Cohen, G.F.C. Rogers, H.I.H. Saravanamuttoo, *Gas Turbine Theory*, Longman Group Ltd, 1996.
- [4] R.E. Jones, Gas turbine engine emissions—problems, progress and future, *Progress in Energy and Combustion Sciences* 4 (1978) 73–113.
- [5] M. Katsuki, T. Hasegawa, The science and technology of combustion in highly preheated air, in: 27th Symposium (International) on Combustion, The Combustion Institute, Pittsburgh, 1998, pp. 3135–3146.
- [6] A.H. Lefebvre, The role of fuel preparation in low-emissions combustion, *Journal of Engineering for Gas Turbines and Power* 117 (1995) 617–655.
- [7] Y. Levy, V. Sherbaum, Parametric study of the FLOXCOM combustor, TAE Report No. 920, Technion, 2003.
- [8] P. Arfi, Reduction of  $\text{NO}_x$  emissions from gas turbines using internal exhaust gas recirculation, PhD Thesis, Technion, Israel, 2002.
- [9] N.K. Rizk, H.C. Mongia, 3-D emission modeling for diffusion flame, rich/lean, and gas turbine combustors, ASME 93-2338, 1993.
- [10] J. Sawyer, *Sawyer's Gas Turbine Engineering Handbook*, 1985.
- [11] J. Tomeczek et al., Gas dynamic abatement of  $\text{NO}_x$  emission from industrial natural gas jet diffusion flames, *Combustion Science and Technology* 105 (1995) 55–65.
- [12] F.J. Verkamp, A.J. Verdow, J.G. Tomlinson, Impact of emission regulations on future gas turbine engine combustor, AIAA Paper 73-1277, 1973.
- [13] A. Wulff, J. Hournouziadis, Technology review of aero-engine pollutant emissions, *Journal of Aerospace Science and Technology* 8 (1997) 557–572.
- [14] J.A. Wunning, *Flameless oxidation von Brennstoff* (German), Thesis, Aachen, 1991.
- [15] J.A. Wunning, J.G. Wunning, Flameless oxidation to reduce thermal  $\text{NO}$ —formation, *Progress in Energy and Combustion Sciences* 23 (1997) 81–94.